Journal of the Oceanographical Society of Japan
Vol. 33, pp. 207 to 218, 1977

A Numerical Study on the Tidal Residual Flow*

Yukio OONISHI**

Abstract: A fundamental mechanism of generation of the tidal residual flow, the steady or quasi-steady flow induced in the tidal current system, is studied by numerical methods. The model basin is a very simple one, a rectangular basin of 5 m×10 m of constant depth and with a cape of 4 m length jutting out at a right angle from the center of the longer side wall. This basin has the same topography as that studied by YANAGI (1976) by means of the hydraulic model experiments.

The steady, circular, horizontal current is found to be induced through the following processes. Horizontal friction at the coast makes the vorticity of vertical component in the oscillating flow. Self-interaction of this flow causes the vorticity transfer to the steady flow in frequency domain. This vorticity transfer is confined in the narrow coastal boundary layer. The steady flow advects the transferred vorticity and makes itself develop fully wide over the bay. In other words, there are two kinds of 'cascade-up', one with regard to time scale and the other with regard to horizontal space scale.

When the tidal range, the tidal period and the horizontal eddy viscosity change under the condition that the model geometry is fixed, the nondimensional parameter which controlls the steady flow is found to be the Reynolds number of the oscillating flow.

1. Introduction

In a coastal current system, as is well known, there are currents which have time scales longer than the period of the principal diurnal or semi-diurnal tide. "Constant flow" or "constant current" is the general term for these currents. The studies on these currents are not so advanced as compared with the studies on tide or the current of the tidal period (hereafter denoted by the tidal flows, or 'TF' in this paper). The first reason for this is that the coastal currents have been studied mainly from the view point of safe navigations and tide preventions. Next reason is that the tidal flows are so prominent in inland seas and bays that it is difficult to measure the weak constant flows accurately. Another reason is that constant flows involve the flows generated by various mechanisms which can not be easily identified quantitatively.

Recently. the long-term variations of the distributions of materials in inland seas or bays have become an important problem in relation to the sea polution. In this situation, hydraulic model experimentalists paid attention to the effective dispersions of materials due to the steady flows induced in their models by the tide (*e.g.* HIGUCHI and YANAGI, 1974). The term "tidal residual flow" (hereafter denoted by 'TRF' in this paper) is given to this flow, which is induced in their hydraulic models by TF itself independently of the heat effects, the wind stress and the inflows from the outer seas. Results of observations in the actual seas have suggested that there are flows similar to TRF observed in the hydraulic model (YAMADA and YANO, 1971), and TRF is now considered as an important component of the constant flows.

There are many problems to be studied on TRF. The first is how much this flow accounts for in the constant flows observed in the actual seas. The second is by what mechanism TRF is generated. The third is how TRF depends on the parameters such as viscosity, tidal range and so on.

In the situation that the estimation of TRF in the observed constant flows can not be made well, the direct comparison of the flows in numerical models and the observed flhws is not a good way to study TRF. One of the ways

* Received Dec. 31, 1976, revised May 18 and accepted Sept. 2, 1977.

** Geophysical Institute, Kyoto University, Kita-shirakawa-oiwakecho, Sakyo-ku, Kyoto 606, Japan

out of the difficulty may be a mutual comparison of results obtained in a numerical model with those in a hydraulic model. If the numerical model is designed well in simulating the phenemena observed in the hydraulic model and the generation mechanism of TRF is understood, the method of calculation used in it may be useful in the simulation of the actual TRF.

It is now considered that large part of the actual TRF is generated in relation to the coastal geometry and 'nonlinear effect' (YAMADA and YANO, 1971; SUGIMOTO, 1975), but the detailed mechanisms have not been found. So, it is better to investigate TRF in a model having a simple coastal geometry than complicated models representing those of the actual seas. From this view point, YANAGI (1976) studied the generation process of TRF by a hydraulic experiment in a model having a simple geometry as shown in Fig. 1. An example of TRF in the model of YANAGI (1976) is shown

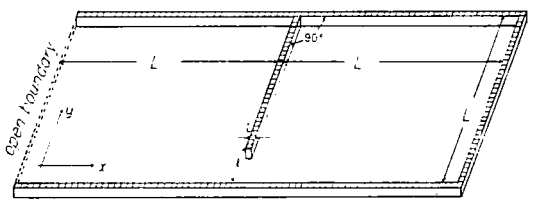

Fig. 1. The model basin (the same as that studied by YANAGI (1976)), of $L=5$ m, $l=1$ m, $l'=14$ cm. The water level oscillation is given at the open boundary by a tide generator in the case of YANAGI, but is prescribed numerically in the case of the present study.

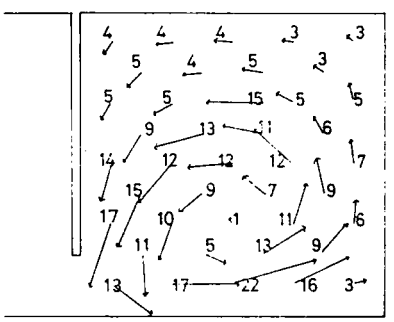

Fig. 2. Residual flow pattern after YANAGI (1976), the same figure as Fig. 6 in his paper except that the nondimensional magnitude of the velocity is written in the figure for the mutual comparison with the results of the numerical model.

in Fig. 2. It is seen that the flow is a circular current, and spreads fully wide over the bay.

The purpose of the present numerical study is to clarify the meanings of the word 'nonlinear effect' on the generation of TRF and the dependence of TRF on two parameters, *i.e.* the tidal range and the horizontal eddy viscocity. This study has been performed parallel to the study of YANAGI (1976) and the model sea of the same topography is treated by method of the numerical study. Calculations are performed by the finite difference method with 35×70 meshes shown in Fig. 1.

2. Preliminary analysis

2.1. *The basic equations and the parameters*

The vertically averaged, horizontally two-dimensional equations are used. The basic equations are written as follows,

$$\frac{\partial u^*}{\partial t^*}+u^*\frac{\partial u^*}{\partial x^*}+v^*\frac{\partial u^*}{\partial y^*}=-g\frac{\partial \zeta^*}{\partial x^*}+\nu_h\Delta_h{}^*u^*+\tau_x{}^*/(h^*+\zeta^*) \quad (1)$$

$$\frac{\partial v^*}{\partial t^*}+u^*\frac{\partial v^*}{\partial x^*}+v^*\frac{\partial v^*}{\partial y^*}=-g\frac{\partial \zeta^*}{\partial y^*}+\nu_h\Delta_h{}^*v^*+\tau_y{}^*/(h^*+\zeta^*) \quad (2)$$

$$\frac{\partial \zeta^*}{\partial t^*}+\frac{\partial}{\partial x^*}\{(h^*+\zeta^*)u^*\}+\frac{\partial}{\partial y^*}\{(h^*+\zeta^*)v^*\}=0 \quad (3)$$

where (x^*, y^*) is the horizontal orthogonal coordinate system shown in Fig. 1, (u^*, v^*) the vertically averaged horizontal velocity in (x^*, y^*) direction, ν_h the coefficient of the horizontal eddy viscosity which represents the diffusing effects of eddies smaller than the mesh size, ζ^* the surface elevation, $(\tau_x{}^*, \tau_y{}^*)$ the bottom stress in (x^*, y^*) direction and h^* the mean depth which is assumed to be constant in this study. To match the condition of the present study to that of the hydraulic model, the Coriolis' terms are not included. The water motion is driven by the water level oscillation of the tidal period T which is given on the open boundary shown in Fig. 1.

TRF in the Yanagi's hydraulic model has

vorticity as clearly shown in Fig. 2. According to Helmholtz's theorem on vortex, this vorticity must be made by the viscous force. So in the numerical model, the vorticity should be made by the terms including ν_h and/or (τ_x^*, τ_y^*). If the bottom stress in the model is taken to be linearly related to the average velocity (u^*, v^*) such as

$$(\tau_x^*, \tau_y^*) = -(2\nu_h/h^*)(u^*, v^*) \quad (4)$$

it can not make the vorticity of vertical component, because h^* is constant. On the other hand, if the bottom stress is assumed that

$$(\tau_x^*, \tau_y^*) = -\gamma_b^2 \sqrt{u^{*2}+v^{*2}}(u^*, v^*) \quad (5)$$

as in the most of past studies on the tidal current system, it is able to make vorticity because of its nonlinear form. But up to now, it is not clear which of these forms is the better expression of the bottom stress in relation to the generation of TRF. In this study, the generation of TRF under the effects of the coastal geometry is treated and the effects of the bottom stress is neglected as the first approximation.

Horizontal viscosity ν_h is so small that the terms including ν_h have smaller values than other terms in Eqs. (1) and (2) except in the coastal oscillatory viscous boundary layer. The layer width $\sqrt{\nu_h T}$ determined by the viscosity ν_h and the tidal period T is an important parameter. The magnitude of nonlinearity is determined by the magnitude of the velocity which is governed by the amplitude a^* of the tide given at the open boundary.

Based on these considerations, the basic equations (1)~(3) are made nondimensional as follows,

$$\frac{\partial u}{\partial t}+\varepsilon\left(u\frac{\partial u}{\partial x}+v\frac{\partial u}{\partial y}\right)=-\lambda\frac{\partial \zeta}{\partial x}+E\Delta u \quad (6)$$

$$\frac{\partial v}{\partial t}+\varepsilon\left(u\frac{\partial v}{\partial x}+v\frac{\partial v}{\partial y}\right)=-\lambda\frac{\partial \zeta}{\partial y}+E\Delta v \quad (7)$$

$$\frac{\partial \zeta}{\partial t}+\frac{\partial}{\partial x}\{(1+\varepsilon\zeta)u\}+\frac{\partial}{\partial y}\{(1+\varepsilon\zeta)v\}=0 \quad (8)$$

where

$$\left.\begin{aligned} &u^*=\varepsilon LT^{-1}u,\ v^*=\varepsilon LT^{-1}v \\ &\zeta^*=\varepsilon h^*\zeta,\ t^*=Tt,\ \varepsilon=a^*/h^* \end{aligned}\right\}$$

$$\left.\begin{aligned} &E=\left(\frac{\sqrt{\nu_h T}}{L}\right)^2,\ \lambda=\left(\frac{T}{L/\sqrt{gh^*}}\right)^2 \end{aligned}\right\} \quad (9)$$

and L is the horizontal scale of the bay shown in Fig. 1. As the basic oscillation of the water level is given uniform on the open boundary, the solution of Eqs. (6)~(8) is prescribed by three parameters ε, λ and E.

The parameter ε defined as the ratio of the tidal amplitude to the depth of the bay is proportional to the Strauhal number† and represents the magnitude of nonlinearily. In the Yanagi's hydraulic model, $a^*=0.5$ cm, $h^*=10$ cm and $\varepsilon=0.05$. Therefore, in this study, the range $\varepsilon=0.0125\sim0.1$ is treated. The parameter E is the square of the ratio of the boundary layer width to the bay scale, and represents the magnitude of the viscous force. It is chosen in the range from 0.0001 to 0.01, which corresponds to the range of ν_h from 0.07 to 7 cm^2s^{-1} with $T=6$ min and $L=5$ m in the hydraulic model. The parameter λ is proportional to the square of the ratio of the tidal period to the fundamental period of the proper oscillation of the external gravity waves in the bay. It is taken to be 5,000, almost the same value as 5,080 in the study of YANAGI (1976). Generally speaking, λ is much larger than 1 in the most of inland seas or bays. λ is not important on the generation of TRF so long as it is much larger than 1 (see Appendix 1). Therefore, the parameters controlling TRF are reduced to ε and E.

2.2. *Analysis*

The tidal flow system is considered to consist of TF and TRF. In order to examine the generation mechanism of TRF, it is convenient to separate the basic equation system into two parts governing TRF and TF. First, each of variables u, v and ζ is expressed as the sum of the time-independent part (TRF) with suffix s and the fluctuating part (TF) with suffix τ such as

$$u=u_S(x, y)+u_T(x, y, t) \quad (10)$$

Substituting u, v and ζ of the form of Eq. (10) into Eqs. (6)~(8) and taking the time average, the following Eqs. (11) and (12) are obtained,

† The Strauhal number is defined as UT/L where U is the order of magnitude of the tidal velocity.

$$\left.\begin{aligned}
&\varepsilon\left(\overline{u_T\frac{\partial u_T}{\partial x}+v_T\frac{\partial u_T}{\partial y}}\right)+\varepsilon\left(u_S\frac{\partial u_S}{\partial x}+v_S\frac{\partial u_S}{\partial y}\right)=-\lambda\frac{\partial\zeta_S}{\partial x}+E\Delta u_S\\
&\varepsilon\left(\overline{u_T\frac{\partial v_T}{\partial x}+v_T\frac{\partial v_T}{\partial y}}\right)+\varepsilon\left(u_S\frac{\partial v_S}{\partial x}+v_S\frac{\partial v_S}{\partial y}\right)=-\lambda\frac{\partial\zeta_S}{\partial y}+E\Delta v_S\\
&\frac{\partial}{\partial x}\{(1+\varepsilon\zeta_S)u_S\}+\frac{\partial}{\partial y}\{(1+\varepsilon\zeta_S)v_S\}+\varepsilon\left\{\frac{\partial}{\partial x}(\zeta_T\overline{u_T})+\frac{\partial}{\partial y}(\overline{\zeta_T v_T})\right\}=0
\end{aligned}\right\}\qquad(11)$$

and

$$\left.\begin{aligned}
&\frac{\partial u_T}{\partial t}+\varepsilon\left(u_S\frac{\partial u_T}{\partial x}+v_S\frac{\partial u_T}{\partial y}+u_T\frac{\partial u_S}{\partial x}+v_T\frac{\partial u_S}{\partial y}\right)=-\lambda\frac{\partial\zeta_T}{\partial x}+E\Delta u_T\\
&\frac{\partial v_T}{\partial t}+\varepsilon\left(u_S\frac{\partial v_T}{\partial x}+v_S\frac{\partial v_T}{\partial y}+u_T\frac{\partial v_S}{\partial x}+v_T\frac{\partial v_S}{\partial y}\right)=-\lambda\frac{\partial\zeta_T}{\partial y}+E\Delta v_T\\
&\frac{\partial\zeta_T}{\partial t}+\frac{\partial u_T}{\partial x}+\frac{\partial v_T}{\partial y}+\varepsilon\left\{\frac{\partial}{\partial x}(\zeta_T u_S+\zeta_S u_T)+\frac{\partial}{\partial y}(\zeta_T v_S+\zeta_S v_T)\right\}=0
\end{aligned}\right\}\qquad(12)$$

where the over-bar denotes the time-average. Eqs. (11) and (12) express the dynamical balance in TRF and TF, respectively. Eqs. (11) show that TRF is accelerated by the horizontal divergence of the Reynolds stress $\left(\varepsilon\left(\overline{u_T\frac{\partial u_T}{\partial x}+v_T\frac{\partial u_T}{\partial y}}\right),\ \varepsilon\left(\overline{u_T\frac{\partial v_T}{\partial x}+v_T\frac{\partial v_T}{\partial y}}\right)\right)$ and the horizontal divergence of excess mass flux $(\varepsilon\overline{\zeta_T u_T},\ \varepsilon\overline{\zeta_T v_T})$.

Excess mass flux can be one of the driving terms of TRF. It is caused by the fact that the phase lag between the tide and the tidal velocity differs from 90°. This phase difference is caused by the viscosity and/or the bottom stress. Therefore, the effect of excess mass flux on TRF is important when the bottom stress have an effect on the tidal phase. HUNT and JOHNS (1963) investigated the case of this type. In their case, TRF has vertical shear and is characterized by the strong current confined in the bottom viscous boundary layer. In the present study, however, TRF of the type discussed by them is not considered because the cases of small viscosity and small bottom stress is concerned and only the vertically averaged flow is concerned. Now, TRF can be treated approximately as a flow having no horizontal divergence. Therefore, TRF is prescribed by the vorticity equation.

Eliminating the pressure terms from Eqs. (11) and (12), we obtain

$$0=\varepsilon F_{TT}+\varepsilon F_{SS}+E\Delta\omega_S\qquad(13)$$

where

$$\begin{aligned}
\omega_S&=\frac{\partial v_S}{\partial x}-\frac{\partial u_S}{\partial y}\\
F_{TT}&=-\frac{\partial}{\partial x}\overline{u_T\omega_T}-\frac{\partial}{\partial y}\overline{v_T\omega_T}\\
F_{SS}&=-\frac{\partial}{\partial x}u_S\omega_S-\frac{\partial}{\partial y}v_S\omega_S
\end{aligned}\qquad(14)$$

and

$$\frac{\partial\omega_T}{\partial t}=E\Delta\omega_T+\varepsilon F_{ST}\qquad(15)$$

where

$$\begin{aligned}
\omega_T&=\frac{\partial v_T}{\partial x}-\frac{\partial u_T}{\partial y}\\
F_{ST}&=-\frac{\partial}{\partial x}(\omega_S u_T)-\frac{\partial}{\partial y}(\omega_S v_T)\\
&\quad-\frac{\partial}{\partial x}(\omega_T u_S)-\frac{\partial}{\partial y}(\omega_T v_S)
\end{aligned}\qquad(16)$$

Eqs. (13) and (15) express the vorticity balances of TRF and TF, respectively. There are three nonlinear terms, F_{TT}, F_{SS} and F_{ST}. The term F_{TT} expresses the nonlinear vorticity transfer from TF to TRF, or a kind of 'cascade-up' of the vorticity in frequency domain. The physical meaning of F_{TT} is as follows: Suppose, for example, that the vorticity of TF is positive and the direction of its velocity is eastwards in the phase of rising tide ($u_T>0$, $\omega_T>0$, $\therefore\ u_T\omega_T>0$). In the ebbing tide, the vorticity must be negative and the direction is westwards

($u_T<0$, $\omega_T<0$, $\therefore$ $u_T\omega_T>0$). Consequently there must be left the eastwards net vorticity flux during one tidal period (*i.e.* $\overline{u_T\omega_T}>0$). The divergence of this net vorticity flux is expressed by the term F_{TT}. The term F_{SS} expresses the re-distribution of the vorticity of TRF by the advection of TRF itself. Eqs. (13) and (15) are coupled through the nonlinear term F_{ST}. In the following sections, the generation mechanism of TRF is investigated based on these vorticity equations.

3. The asymptotic solutions in the limit of $\varepsilon\to 0$

In this section, the asymptotic solution in the limit of weak nonlinearity ($\varepsilon\to 0$) is considered as the first step. The variables are in the following orders of magnitude on ε, *i.e.* $u_T=O(1)$, $v_T=O(1)$, $\omega_T=O(1)$. Substituting these into the expressions of F_{TT}, F_{SS} and F_{ST} in Eqs. (14) and (16), it is found that $u_S=O(\varepsilon)$, $v_S=O(\varepsilon)$, $\omega_S=O(\varepsilon)$, $F_{TT}=O(1)$, $F_{SS}=O(\varepsilon^2)$ and $F_{ST}=O(\varepsilon)$. Therefore, the lowest order equations on ε are obtained as follows,

$$0=\varepsilon F_{TT}+E\Delta\omega_S \tag{17}$$

and

$$\frac{\partial\omega_T}{\partial t}=E\Delta\omega_T \tag{18}$$

Eq. (17) expresses that the transferred vorticity from TF to TRF balances locally with the viscous dissipation of the vorticity of TRF; Eq. (18) expresses that the vorticity of TF is generated by the horizontal viscous stress.

Now, let us examine the distribution of F_{TT} for small value of E. Based on Eq. (18), the solution for TF must consist of the irrotational interior solution, which is independent of E, and the viscous correction $(\tilde{u},\tilde{v})=(\partial\tilde{\varphi}/\partial y,\ -\partial\tilde{\varphi}/\partial x)$, which decays exponentially from the coast into the interior region. Taking the coordinates ξ and η such that they are normal and parallel to the coast line, respectively, the equation and the boundary conditions governing $\tilde{\varphi}$ are written as

$$\frac{\partial}{\partial t}\frac{\partial^2\tilde{\varphi}}{\partial\xi^2}=E\frac{\partial^4\tilde{\varphi}}{\partial\xi^4}$$

$$\tilde{\varphi}=0,\ \frac{\partial\tilde{\varphi}}{\partial\xi}R_e[-V(\eta)e^{2\pi it}]\quad\text{at }\xi=0$$

$$\tilde{\varphi}\to 0\ \text{as}\ \xi\to\infty \tag{19}$$

where $V(\eta)$ is the irrotational velocity of TF at the coast. Solution of Eq. (19) is

$$\tilde{\varphi}=R_e\left[-\sqrt{\frac{E}{\pi}}\frac{V(\eta)}{1+i}\times\left\{1-\exp\left(-\sqrt{\frac{\pi}{E}}(1+i)\right)\right\}e^{2\pi it}\right] \tag{20}$$

From this solution, it is easily shown that F_{TT} has large values only in the viscous boundary layer whose width is proportional to $\sqrt{E}$ and that it has the order of magnitude proportional to $1/\sqrt{E}$. Therefore, the total vorticity transferred per unit length of the coast line or the integral of F_{TT} with respect to ξ approaches a non-zero value (independent of E) as $E\to 0$.

Numerical calculations are made for two finite values of E such that $E=0.01$ and $E=0.001$. First, TF is obtained by solving Eq. (18) (see Appendix 2) and then F_{TT} is calculated. Figs. 3a and b show F_{TT} in cases of $E=0.01$ and $E=0.001$, respectively. It is seen that F_{TT} is confined in a coastal boundary layer near the tip of the cape and that F_{TT} is positive in the inner bay but is negative in the outer sea. This distribution of F_{TT} originates from the coastal geometry of the cape. TRF is calculated from Eq. (17) (see Appendix 2) in both cases and is shown in Figs. 4a and b.

According to the sign of F_{TT}, the calculated

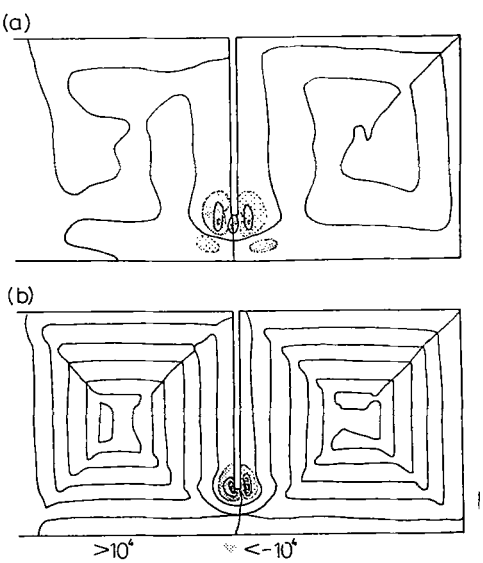

Fig. 3. Patterns of the vorticity transfer F_{TT} in the limiting case of $\varepsilon\to 0$, (a) with $E=0.01$, (b) with $E=0.001$. Contour interval is 5×10^4.

TRF rotates anticlockwise in the inner bay and clockwise in the outer sea. This sense of rotation is consistent with that of the hydraulic model experiment (Fig. 2). The patterns of TRF in the present model, however, do not resemble well to those in the hydraulic model, *i.e.* the center of the vortex in the numerical model is closer to the tip of the cape than that in the hydraulic model. Confinement of the calculated flow in the neighbourhood of the tip is the direct reflection of the distribution of F_{TT}, because F_{TT} locally balances with the viscous dissipation term in the limit of $\varepsilon \to 0$.

4. Cases of finite amplitude

It is considered that the main discrepancy between the results in the numerical model mentioned above (the case of $\varepsilon \to 0$) and those in the hydraulic model, is attributed to the finiteness of ε. The terms F_{SS} and F_{ST} are both the second-order quantities on ε in Eqs.

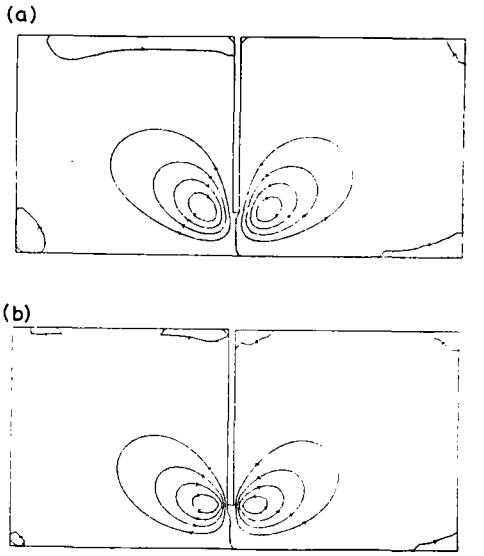

Fig. 4. Calculated patterns of TRF in the limiting case of $\varepsilon \to 0$, where (a) and (b) correspond to Fig. 3a and b, respectively.

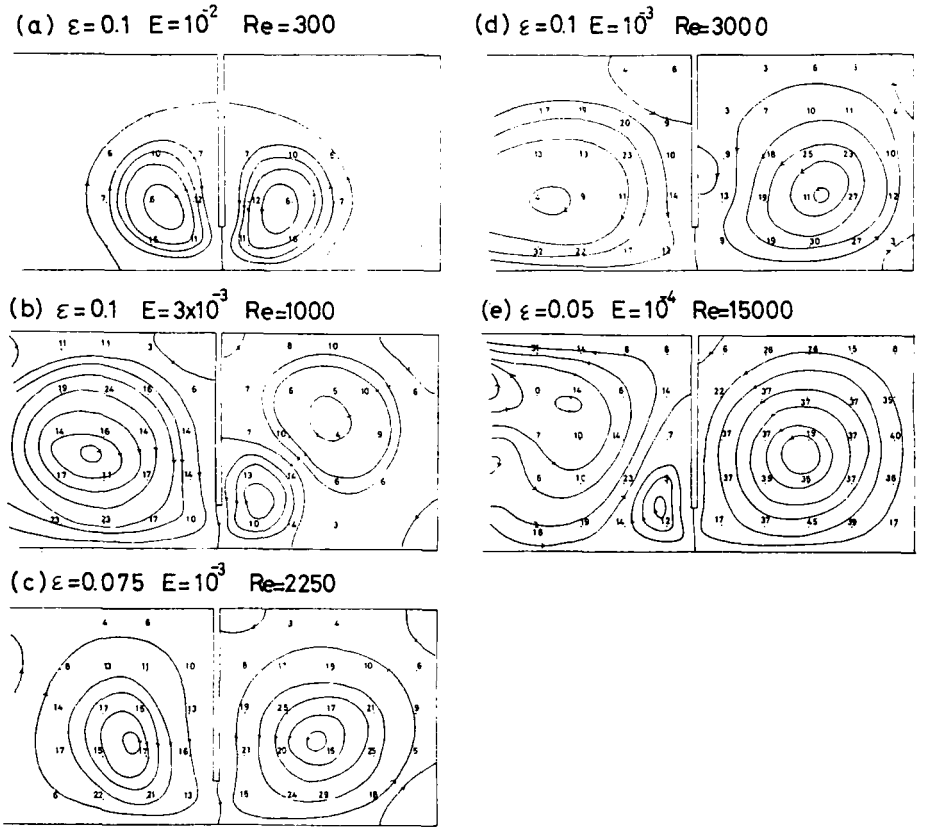

Fig. 5. Patterns of TRF by the primitive method for various combinations of two parameters ε and E.

(13) and (15), respectively. As seen in these equations, F_{ST} would affect TF and so vary F_{TT} via TF. If F_{TT} would spread fully wide over the bay under the effect of F_{ST}, TRF would do so. On the other hand, F_{SS} directly affects TRF. The question is which is the more effective of these two terms F_{ST} and F_{SS}.

To solve this problem, the time integration of Eqs. (6)~(8) are performed by the primitive method (see Appendix 2). Since no separation of TF and TRF is made in this method, they are separated later by averaging the calculated flow with time over one tidal period. Starting from the state of rest, TRF approaches a steady state in 4~20 tidal periods, whose length depends on the values of the parameters. The resulting patterns of TRF are shown in Fig. 5. Numerals in the figures denote the magnitudes of the nondimensional velocities. In the case of Fig. 5a, the flow pattern resembles that in the previous case of the limit of $\varepsilon \to 0$, but in other cases of Fig. 5c~e, the flow develops fully wide over the bay as that in the hydraulic model. Discussions on this difference in the flow pattern will be made later. Now, let us examine the vorticity balance of TRF. For example, distribution of F_{TT}, F_{SS} and the viscous dissipation term $(E/\varepsilon)\Delta\omega_S$ in the case corresponding to Fig. 5c are shown in Figs. 6a, b and c, respectively. In the case of the finite amplitude as well as in the case of the limit of $\varepsilon \to 0$, F_{TT} is large only in the neighbourhood of the tip of the cape. As shown in Fig. 6b, the advection term F_{SS} has the opposite sign to F_{TT} and the similar absolute value to it. Fig. 6c shows that the vorticity of TRF is dissipated on the surrounding coast of the bay. As seen from the distribution of F_{TT} in Fig. 6a, the development of TRF fully wide over the bay is not caused by the wide spreading of the large value of F_{TT} over the bay. The transferred vorticity is not dissipated locally, but advected to the coast of the inner bay, and dissipated there. Thus the full development is attained.

The distributions of F_{TT} for all cases are shown in Fig. 7. In some cases, *e.g.* Fig. 7e, F_{TT} shows rather complicated pattern. But the fact that it has two peaks in the neighbourhood of the tip of the cape is preserved as in the limiting case of $\varepsilon \to 0$. It implies that the interaction term F_{ST} is not so important even in the case of finite amplitude, and that F_{SS} must be essentially important to the wide spreading of TRF.

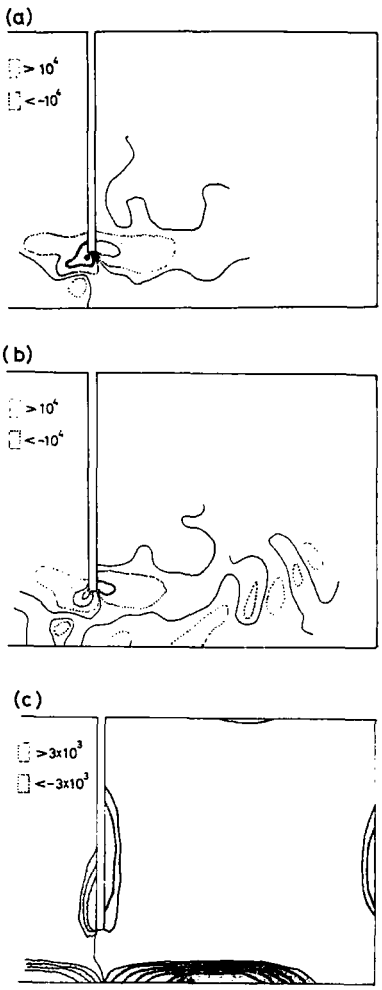

Fig. 6. The balance of terms in TRF, where (a), (b) and (c) show F_{TT}, F_{SS} (contour intervals are both 5×10^{4}), and $(E/\varepsilon)\Delta\omega_S$ (contour interval 3×10^{3} and contours for zero-value excluded), respectively.

Let us examine this idea by solving the vorticity equations neglecting the interaction term F_{ST}, *i.e.* by solving Eqs. (13) and (17). As Reynolds number R_e† is proportional to ε/E,

† The nondimensional velocity u_M of TF at the mouth of the bay is determined as $u_M=2\pi S/l$ with the area S of the bay and the width l of the mouth. In this study, u_M is about 30 with $S=1$ and $l=0.2$. Using u_M, the scale of the bay L and the horizontal viscosity ν_h, Reynolds number R_e is written as $R_e=(\varepsilon u_M LT^{-1})L/\nu_h$ and therefore as $R_e=u_M\varepsilon/E$.

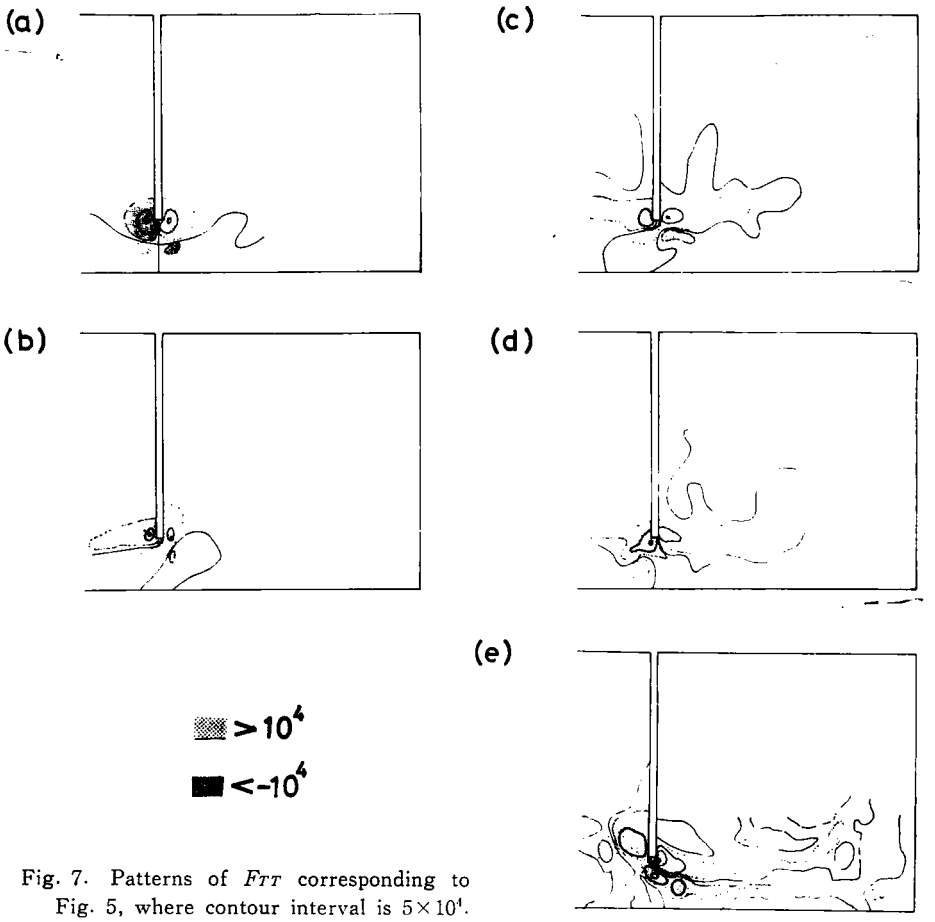

Fig. 7. Patterns of F_{TT} corresponding to Fig. 5, where contour interval is 5×10^4.

Eq. (13) is rewritten as

$$0=F_{TT}+F_{SS}+u_M R_e^{-1}\Delta\omega_S \qquad (21)$$

Now, a system of Eqs. (18) and (21) is to be solved and the basic parameters are two, *i.e.* E and R_e. It is, however, shown that the important parameter is only one, *i.e.* R_e.

When the viscosity parameter E varies, as shown in Figs. 3a and b, the distribution of F_{TT} varies. In the case of the finite amplitude, however, the transferred vorticity is advected out of the viscous boundary layer. Therefore, changes of the distribution pattern of F_{TT} are not important. Important is the integrated value of F_{TT} over the boundary layer width. On the other hand, as shown in the previous section, this integral approaches a constant value in the limit of $E\to0$. From these facts, the parameter E is not important to determine TRF so long as E is small.

Numerical calculations are made based on Eq. (21) (see Appendix 2) for several values of R_e under the condition that F_{TT} is fixed to that shown in Fig. 3a for the case of $E=0.001$. The change of TRF pattern with R_e is shown in Figs. 8a~f. In the case of $R_e=375$, the center of the vortex is situated near the tip and the flow pattern resembles that of $R_e\to0$ ($\varepsilon\to0$) discussed in the last section. As R_e becomes large to 750, the vortex pattern becomes to break up into two parts which have the opposite senses of rotation each other. In the case of $R_e=1{,}125$, the center of the vortex appears in the interior region of the bay. When $R_e=1{,}500$, the flow spreads wide over the bay. As the horizontal content of the bay is limited, it is considered that the flow can not grow unlimetedly even if R_e becomes larger. In the case of $R_e=2{,}250$ and 3,000, the flow intends to meander. It suggests that TRF may become

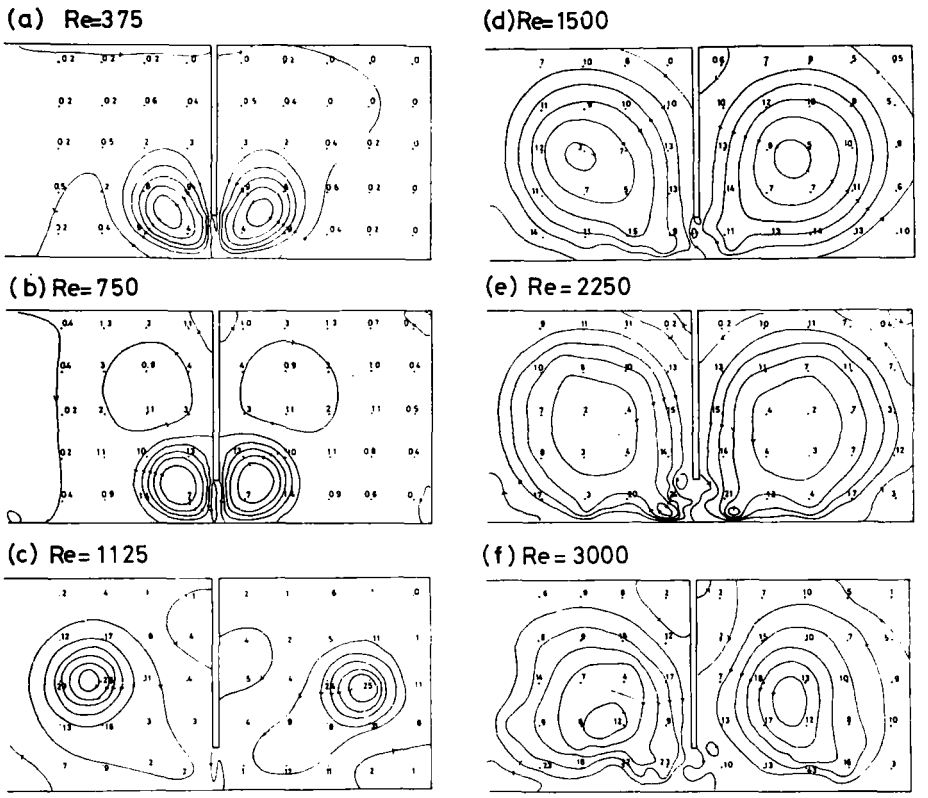

Fig. 8. The change of TRF pattern with R_e, obtained by the method neglecting F_{ST}.

unstable for the larger values of R_e. Considering these facts, the value of R_e between 1,125 and 1,500 may be 'critical' to the condition whether TRF spreads over the bay. Comparing Fig. 8 and Fig. 5, it is seen that this change of TRF with R_e explain well the change obtained by the primitive method. Now it is concluded that the spread of TRF is controlled by the value of R_e.

Finally, the ratio K of the total kinetic energy of TRF to that of TF as a function of R_e is shown in Fig. 9. Because the total kinetic energy of TF oscillates with time, its maximum value with respect to time is taken as the denominator. It is seen from Fig. 9 that the kinetic energy of TRF is larger than that of TF for a Reynolds number larger than about 1,000. It seems that $K(R_e)$ becomes larger almost monotonously with R_e except that it stagnates near the 'critical' Reynolds number. The dimensional kinetic energy of TRF is proportional to $\varepsilon^2 K(u_M \varepsilon/E)$ and increases monotonously and more rapidly than that of TF with the tidal range.

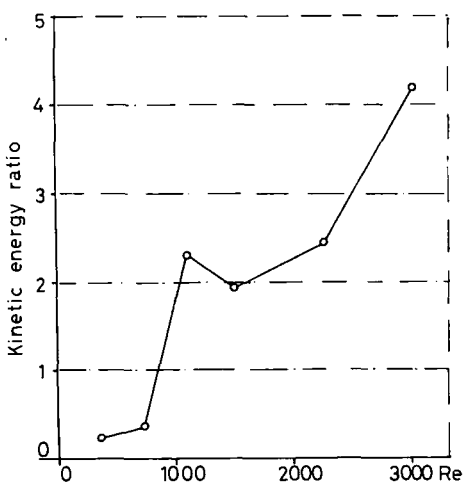

Fig. 9. The ratio of the integrated kinetic energy of TRF to that of TF. The integrations are made over the inner bay.

5. Discussion

The vorticity transfer F_{TT} from TF to TRF occurs in the narrow viscous boundary layer. This is a kind of 'cascade-up' with regard to

time scale. The fully wide spreading of TRF in the bay is attained by the advection of the vorticity of TRF by TRF itself. This is also a kind of 'cascade-up' with respect to space scale. These two kinds of 'cascade-up' are the contents of the 'nonlinear effect' on the generation of TRF. Therefore, even if TRF with a large horizontal scale is concerned, the process with small spatial scale (*i.e.* the generation of the vorticity in the boundary layer along the coast) are important in its generation process. The numerical model of TRF must have a small mesh size which can resolute this process, because this process can not be parameterized by a so-called eddy viscosity.

Viscosity plays two kinds of roles. One is a role in the generation of the vorticity of TF in the boundary layer. It should be noted that though this process is fundamental in the generation of TRF itself the value of the viscosity coefficient is not necessarily important in the generation. The width of the boundary layer and the strength of the shear of the velocity are proportional to $\sqrt{\nu_h}$ and $1/\sqrt{\nu_h}$, respectively. So, the total amount of the vorticity transferred to TRF does not so strongly depend on ν_h.

Viscosity has the other role as a dissipating factor in the vorticity balance in TRF. Reynolds number which prescribes this balance controlls the pattern and the strength of the steady flow. In this study, the bottom stress is not included. In an actual shallow sea near the coast, however, the bottom friction may have a larger effect than the horizontal friction as a dissipating factor. In such a case, Reynolds number should be re-defined from the balance between the advective terms and the bottom friction terms. Corresponding to two expressions of the bottom friction in Eqs. (5) and (4), Reynolds number has two forms as $R_e=h^*/(L\gamma_b^2)$ and $R_e=\varepsilon u_M h^{*2}/(2\nu_v T)$, respectively. The former is independent of the non-dimensional tidal amplitude ε, while the latter is proportional to it. The followings should be noted here:

1. In the former case, the pattern of TRF would not change with ε but its energy would change proportional to ε^2.
2. In the latter case, the pattern of TRF would change with ε and the so-called power dependence of the kinetic energy on ε may be larger than 2 as shown in Fig. 9.

In any case, TRF becomes stronger with the tidal amplitude. From this reason, TRF in the actual sea is not exactly steady, but it should have long-term variations corresponding to the amplitude oscillation of the tide.

The bottom friction may induce a vertial shear in the flow. The flow with the horizontal circulation and the vertical shear may induce the secondary vertical flow through a process which is analogous to the Ekman suction. These problem will be investigated in the following paper.

Acknowledgements

I want to express my thanks to Prof. H. KUNISHI and Dr. N. IMASATO of Kyoto University for their encouragements and productive discussions. I also thank to Mr. T. YANAGI for his valuable suggestions based on the facts in the hydraulic model experiments. The numerical calculations were carried out on a Facom 230-75 of the Data Proceeding Center of Kyoto University.

References

HIGUCHI, H. and T. YANAGI (1974): On the hydraulic model experiment on the diffusion due to the tidal current (IV). Disaster Prev. Res. Inst. Annuals of Kyoto Univ., **17B**, 647-655 (in Japanese).

HUNT, J. N. and B. JOHNS (1963): Current induced by tides and gravity waves. Tellus, **15**, 343-351.

SUGIMOTO, T. (1975): Effect of boundary geometries on tidal currents and tidal mixing. J. Oceanogr. Soc. Japan, **31**, 1-31.

YANAGI, T. (1976): The fundamental study of the tidal residual circulation. J. Oceanogr. Soc. Japan, **32**, 199-208.

YAMADA, T. and Y. YANO (1971): On occurrence of constant and quater-diurnal currents by the topographical effect. Report of Hydrographic Researches, b, pp. 63-77 (in Japanese).

Appendix 1

If λ is much larger than 1, the variables are expressed as the power series of $1/\lambda$ as

$$\zeta=\zeta^{(0)}+\left(\frac{1}{\lambda}\right)\zeta^{(1)}+\left(\frac{1}{\lambda}\right)^2\zeta^{(2)}+\cdots.$$

Substituting u, v and ζ of the forms as this into Eqs. (6)~(8), the following 0-th order equations are obtained,

$$\frac{\partial \zeta^{(0)}}{\partial x}=\frac{\partial \zeta^{(0)}}{\partial y}=0,\quad \frac{\partial u^{(0)}}{\partial x}+\frac{\partial v^{(0)}}{\partial y}=-\frac{\zeta^{(0)}}{1+\varepsilon\zeta^{(0)}}\frac{\partial \zeta^{(0)}}{\partial t}$$

$$\frac{\partial u^{(0)}}{\partial t}+\varepsilon\left(u^{(0)}\frac{\partial u^{(0)}}{\partial x}+v^{(0)}\frac{\partial u^{(0)}}{\partial y}\right)=-\frac{\partial \zeta^{(1)}}{\partial x}+E\Delta u^{(0)}$$

$$\frac{\partial v^{(0)}}{\partial t}+\varepsilon\left(u^{(0)}\frac{\partial v^{(0)}}{\partial x}+v^{(0)}\frac{\partial v^{(0)}}{\partial y}\right)=-\frac{\partial \zeta^{(1)}}{\partial y}+E\Delta v^{(0)}$$

These equations mean that the 0-th order surface elevation $\zeta^{(0)}$ is independent of x and y and that the divergence of the 0-th order velocity $(u^{(0)}, v^{(0)})$ is prescribed by $\zeta^{(0)}$. In other words, $\zeta^{(0)}$ can be interpreted as a vertical displacement of a rigid lid over the sea. In this sense, this system is a kind of a 'rigid-lid' approximation. The parameter λ does not appear in the resulting system, *i.e.* λ does not work on the flow.

Appendix 2

1) The method for solving Eq. (18):

The horizontal velocity (u_T, v_T) can be expressed as follows

$$\left.\begin{aligned} u_T&=-\frac{\partial \phi}{\partial x}+\frac{\partial \psi}{\partial y}\\ v_T&=-\frac{\partial \phi}{\partial y}-\frac{\partial \psi}{\partial x}\end{aligned}\right\}\quad \text{(A-1)}$$

where ϕ and ψ are the velocity potential and the stream function, respectively. As λ is much larger than 1, the divergence $\frac{\partial u_T}{\partial x}+\frac{\partial v_T}{\partial y}=-\Delta\phi$ is prescribed as a function of time only as shown in Appendix 1. If we consider the limiting case of $\varepsilon\to 0$, we obtain the following system of equations.

$$\left.\begin{aligned} &\Delta\phi=2\pi\sin 2\pi t\\ &\Delta\psi=-\omega_T,\quad \frac{\partial \omega_T}{\partial t}=E\Delta\omega_T\\ &\text{with the boundary conditions as}\\ &-\frac{\partial \phi}{\partial x}+\frac{\partial \psi}{\partial y}=-\frac{\partial \phi}{\partial y}-\frac{\partial \psi}{\partial x}=0\\ &\qquad\text{at the coast}\\ &\frac{\partial \psi}{\partial x}=\frac{\partial \psi}{\partial y}=0\quad\text{at the open boundary}\end{aligned}\right\}\quad \text{(A-2)}$$

Because the system is linear, the solution is expressed as the forms

$$\left.\begin{aligned} \phi&=\phi_1\sin 2\pi t+\phi_2\cos 2\pi t\\ \omega_T&=\omega_1\sin 2\pi t+\omega_2\cos 2\pi t\\ \psi&=\psi_1\sin 2\pi t\end{aligned}\right\}\quad \text{(A-3)}$$

Substituting Eqs. (A-3) into Eqs. (A-2), we obtain

$$\left.\begin{aligned} &\Delta\phi_1=2\pi\\ &\Delta\psi_1=-\omega_1,\quad \Delta\psi_2=-\omega_2\\ &-2\pi\omega_1=E\Delta\omega_2,\quad 2\pi\omega_2=E\Delta\omega_1\\ &-\frac{\partial \phi_1}{\partial x}+\frac{\partial \psi_1}{\partial y}=-\frac{\partial \phi_1}{\partial y}-\frac{\partial \psi_1}{\partial x}\\ &\quad=\frac{\partial \psi_2}{\partial y}=\frac{\partial \phi_2}{\partial x}=0\quad\text{at the coast}\\ &\frac{\partial \psi_1}{\partial x}=\frac{\partial \psi_1}{\partial y}=\frac{\partial \psi_2}{\partial x}=\frac{\partial \psi_2}{\partial y}=0\\ &\qquad\text{at the open boundary}\end{aligned}\right\}\quad \text{(A-4)}$$

Taking a usual finite difference versions of these equations, we obtain a system of simultaneous linear equations. The resulting system is solved by an iterative method.

2) The method for solving Eq. (7) or Eq. (13):

With the stream function ψ_S, u_S and v_S can be expressed as

$$u_S=\frac{\partial \psi_S}{\partial y},\quad v_S=-\frac{\partial \psi_S}{\partial x}$$

Eq. (13) and the corresponding boundary condition are rewritten as

$$\left.\begin{aligned} &\frac{\partial}{\partial x}\left(\omega_S\frac{\partial \psi_S}{\partial y}\right)-\frac{\partial}{\partial y}\left(\omega_S\frac{\partial \psi_S}{\partial x}\right)\\ &\quad=F_{TT}+\frac{E}{\varepsilon}\Delta\omega_S\\ &\Delta\psi_S=-\omega_S\\ &\frac{\partial \psi_S}{\partial x}=\frac{\partial \psi_S}{\partial y}=0\quad\text{at the boundary}\end{aligned}\right\}\quad \text{(A-5)}$$

When Eq. (17) is concerned, the left hand side of the first equation of (A-5) is neglected. Then the system is linear and it is solved by a similar method used to solve Eq. (18). When Eq. (13) is concerned, the first equation of (A-5) is replaced by

$$\frac{\partial \omega_S}{\partial t}+\frac{\partial}{\partial x}\left(\omega_S\frac{\partial \psi_S}{\partial y}\right)-\frac{\partial}{\partial y}\left(\omega_S\frac{\partial \psi_S}{\partial x}\right)$$
$$=F_{TT}+\frac{E}{\varepsilon}\Delta\omega_S$$

The resulting system is integrated with respect to time t by a finite difference method till the solution converges to a quasi-steady state.

3) The method for solving Eqs. (6)~(8):

Eqs. (6)~(8) and the boundary conditions are replaced by its finite difference versions, which is integrated with respect to time. The time integration is performed by a semi-implicit method. It is as follows. If the variables at $t=n\delta t$ is expressed with overscript n, *e.g.* u^n *etc.*, Eqs. (6)~(8) are transformed to

$$\left.\begin{aligned}
&\frac{u^{n+1}-u^{n-1}}{2\delta t}+\varepsilon\left(u^n\frac{\partial u^n}{\partial x}+v^n\frac{\partial u^n}{\partial y}\right)\\
&=-\alpha\lambda\frac{\partial\zeta^{n+1}}{\partial x}-(1-\alpha)\lambda\frac{\partial\zeta^{n-1}}{\partial x}+E\Delta u^{n-1}\\
&\frac{v^{n+1}-v^{n-1}}{2\delta t}+\varepsilon\left(u^n\frac{\partial v^n}{\partial x}+v^n\frac{\partial v^n}{\partial y}\right)\\
&=-\alpha\lambda\frac{\partial\zeta^{n+1}}{\partial y}-(1-\alpha)\lambda\frac{\partial\zeta^{n-1}}{\partial x}+E\Delta v^{n-1}
\end{aligned}\right\}\quad\text{(A-6)}$$

$$\left.\begin{aligned}
&\frac{\zeta^{n+1}-\zeta^{n-1}}{2\delta t}+\frac{\partial}{\partial x}[(1+\varepsilon\zeta^n)\{\alpha u^{n+1}\\
&+(1-\alpha)u^{n-1}\}]+\frac{\partial}{\partial y}[(1+\varepsilon\zeta^n)\\
&\times\{\alpha v^{n+1}+(1-\alpha)v^{n-1}\}]=0
\end{aligned}\right|$$

These equations are solved with respect to u^{n+1}, v^{n+1} and ζ^{n+1} by an iterative method, and a step of time integration is performed. The time integration is made by continueing these steps. A comparison of the results with $\alpha=0.5$ and $\alpha=0.6$ (in the case of $\varepsilon=0.1$ and $E=0.001$) showed that the results are similar each other but the latter result is a little smooth horizontally. The other cases of the runs are performed under $\alpha=0.6$. The advantage of the method when $\alpha\geqq 1/2$ is that *CPU* time is saved in the cases that λ is much larger than 1 as the *C-F-L*'s condition $\delta t\leqq\delta x\sqrt{2\lambda}$ (δx expresses the horizontal mesh size) with regard to the external gravity waves is not necessarily satisfied.

潮汐残差流に関する数値研究

大　西　行　雄

要旨: 潮汐流系の内部で作られる定常流または準定常流，すなわち潮汐残差流の基本的発生機構を数値的手法によって研究した．模型海は，水深が一定の5m×10mの矩形で，長辺の中央から長さ4mの岬が長辺に直角に突き出しているという簡単な地形を持っている．この模型海は，柳（1976）が水理模型手法によって研究した模型と同型である．

定常な水平循環流系が次のような過程を経て作られることがわかった．海岸での水平摩擦によって，振動流中に鉛直成分をもつ渦度が作られる．この振動流の自己相互作用によって振動数空間で定常流への渦度の転換がひき起こされる．この転換は狭い沿岸境界層の中で起こる．定常流に転換された渦度の定常流による移流，言い換えれば定常流の自己相互作用によって定常流それ自身が湾内に広く発達する．時間規模に関するものと，空間規模に関するものの，二種のいわゆる「カスケードアップ」の過程が潮汐残差流を作る．

地形を固定し，潮位差，潮汐周期，水平渦動粘性係数を変化させると，潮汐残差流の強さとそのパターンは潮流のレイノルズ数によって規定されることが示された．

* 京都大学理学部地球物理学教室，
〒606 京都市左京区北白川追分町